Journal of Hydrology 556 (2018) 944–960

Contents lists available at ScienceDirect

Journal of Hydrology

journal homepage: www.elsevier.com/locate/jhydrol

Circulation pattern-based assessment of projected climate change for a catchment in Spain

Hoshin V. Gupta [a], Gonzalo Sapriza-Azuri [b,c,*], Jorge Jódar [c], Jesús Carrera [c]

[a] Department of Hydrology and Water Resources, The University of Arizona, Tucson, AZ, USA
[b] Departamento del Agua, Centro Universitario Región Litoral Norte, Universidad de la República Uruguay, Salto, Uruguay
[c] GHS UPC-CSIC, Institute of Environmental Assessment and Water Research (IDAEA), CSIC, Barcelona, Spain

ARTICLE INFO

Article history:
Available online 17 June 2016

Keywords:
Climate impact assessment
Hydro-Climatology
ACPology
Atmospheric circulation patterns
Number of Rainy Days
Probability of Rain
Wet Day Amount
Temperature
Spain

ABSTRACT

We present an approach for evaluating catchment-scale hydro-meteorological impacts of projected climate change based on the atmospheric circulation patterns (ACPs) of a region. Our approach is motivated by the conjecture that GCMs are especially good at simulating the atmospheric circulation patterns that control moisture transport, and which can be expected to change in response to global warming. In support of this, we show (for the late 20th century) that GCMs provide much better simulations of ACPs than those of precipitation amount for the Upper Guadiana Basin in central Spain. For the same period, four of the twenty GCMs participating in the most recent (5th) IPCC Assessment provide quite accurate representations of the spatial patterns of mean sea level pressure, the frequency distribution of ACP type, the 'number of rainy days per month', and the daily 'probability of rain' (they also reproduce the *trend* of 'wet day amount', though not the actual magnitudes). A consequent analysis of projected trends and changes in hydro-climatic ACPology between the late 20th and 21st Centuries indicates that (1) actual changes appear to be occurring faster than predicted by the models, and (2) for two greenhouse gas emission scenarios (RCP 4.5 and RCP 8.5) the expected decline in precipitation volume is associated mainly with a few specific ACPs (primarily directional flows from the Atlantic Ocean and Cantabric Sea), and with decreasing probability of rain (linked to increasing temperatures) rather than wet day amount. Our approach is a potentially more insightful alternative for catchment-scale climate impacts assessments than the common approach of statistical downscaling and bias correction.

© 2016 Elsevier B.V. All rights reserved.

1. Introduction

1.1. Goals of this paper

At Mediterranean latitudes, 21st century simulations by General Circulation Models (GCMs) project increases in temperature and reductions in rainfall, and this process may have already begun (Lionello et al., 2014). These changes can be expected to severely impact water resources management, requiring the development of hydrological models for planning. Ideally, GCM projections of hydrometeorological fields would be the primary source of information for local- and regional-scale hydrological studies. However, such models typically provide poor simulations of the magnitude of daily precipitation, the primary hydrometeorological field required for hydrological analysis. It is common, therefore, to apply bias corrections, often along with statistical or dynamical downscaling, to the GCMs outputs (Wood et al., 2002, 2004; Maurer, 2007; Fowler et al., 2007; Piani et al., 2010; Johnson and Sharma, 2012; Wi et al., 2012). Such corrections implicitly assume that the spatial and temporal patterns of hydroclimatic variables (notably, temperature and precipitation) will remain invariant.

In this paper, we take the view that it is reasonable to assume that GCMs are especially good at simulating *atmospheric circulation*, which is the underlying control on moisture transport, and thereby rainfall. Therefore, it is also natural to presume that GCMs can be expected to remain equally good at simulating the changes in atmospheric circulation that can be expected to occur in response to global warming. This capability is especially relevant for Mediterranean latitudes, where changes in rainfall are driven largely by changes in atmospheric circulation (Xoplaki et al., 2012). Therefore, the focus of this paper is an approach to investigating local- and regional-scale hydrologic impacts that is based on the ability of GCMs to simulate the atmospheric circulation

* Corresponding author at: Departamento del Agua, Centro Universitario Región Litoral Norte, Universidad de la República Uruguay, Salto, Uruguay.
E-mail addresses: gsapriza@unorte.edu.uy, gsapriza@gmail.com (G. Sapriza-Azuri).

http://dx.doi.org/10.1016/j.jhydrol.2016.06.032
0022-1694/© 2016 Elsevier B.V. All rights reserved.

patterns (ACPs) for the region of interest (Randall et al., 2007; Sheridan and Lee, 2010; Lee and Sheridan, 2011).

While our goal is a general and relatively simple methodology for assessment of projected climate change (i.e., one that is simple enough to be easily applied for water resources assessment), we develop and illustrate our approach for the ~16,000 km^2 Upper Guadiana Basin in Central Spain. In doing so, we evaluate how local climate variables can be expected to change due to projected shifts in climate during the 21st century. The climate variables of interest include the daily minimum, average and maximum temperatures (*TMin*, *TAvg* and *TMax*), and the occurrence (or not) and amount of daily precipitation (*PVol*), averaged over the basin, all of which are important for water resources assessments (Piao et al., 2010; Sivakumar, 2011).

To ensure some degree of generality to our findings, and because the quality of climate simulations at a specific location varies from model to model (Brekke et al., 2008; Pierce et al., 2009; Dominguez et al., 2010), we examine and assess the climate change projections provided by a suite of 20 General Circulation Models (GCMs) participating in the most recent (5th) assessment conducted by the Intergovernmental Panel on Climate Change (IPCC); the projections are available from the website of Phase 5 of the Coupled Model Intercomparison Project (CMIP5 http://cmip-pcmdi.llnl.gov/cmip5/) (Taylor et al., 2011).

Specifically we seek to answer the following questions:

(Q1) Which of the hydro-meteorological variables (precipitation and temperature) needed for catchment scale assessments are simulated well enough by GCMs that they can be used to assess the impacts of climate variability/change?
(Q2) Which of the available GCMs provide better simulations of the historical patterns of atmospheric circulation, precipitation and temperature over the region of interest?
(Q3) What inferences can be made (from available GCM simulations) about potential future trends in the hydro-meteorological variables of interest?
(Q4) What inferences can be made (from available GCM simulations) about potential future changes in annual climatology (pattern of mean monthly values) and ACPology (pattern of mean values per ACP)?

Regarding potential future changes in climate, this study will examine two emission scenarios (RCP 4.5 and RCP 8.5; see Section 4) considered under the most recent IPCC climate change assessment (IPCC, 2013).

1.2. Background and motivation

The hydroclimatic information provided by ACPs has found a wide range of application in many fields (e.g. precipitation, climate change, pollutant episode, mortality, etc.) (Bardossy and Plate, 1992; Esteban et al., 2005; Stahl et al., 2006; Huth et al., 2008; Demuzere et al., 2009; Lee and Sheridan, 2011). Recent studies (Bárdossy and Pegram, 2011; Sapriza-Azuri et al., 2013; Haberlandt et al., 2014) have illustrated the usefulness of incorporating ACPs in downscaling and bias correction methodologies. In particular Sapriza-Azuri et al. (2013) demonstrated that several aspects of the spatio-temporal non-stationarity of catchment scale spatially-distributed rainfall fields can be reproduced by decomposing the rainfall generating process into several, time-stationary, stochastic rainfall generating processes (SRGPs). In this manner, changes in the frequencies of different types of precipitation generating mechanisms (frontal and convective), and interactions between the mesoscale atmospheric patterns and local topography (orographic effects) can be accounted for. In other words, their approach is based on the reasonable assumption that differences in spatial patterns and intensities of precipitation can (at least in part) be explained by differences in the directions and intensities of the winds, patterns of atmospheric pressure, time of year (coded through temperature), and source locations of moisture associated with different ACPs.

Therefore, instead of downscaling precipitation based on statistical bias correction or dynamical modeling, the Sapriza-Azuri et al. (2013) method uses local precipitation gauge data, and information regarding topographic elevation, to develop several time-stationary SRGPs – one for each of several ACP types (discussed later) and time of year (coded in terms of season). Each SRGP can then be used to generate multiple stochastic realizations of daily rainfall fields (at arbitrarily high spatial resolution) that preserve the observed spatial covariance, and the drift in intensity associated with topography.

To apply the SRGP method to catchment scale hydrological modeling and water resources evaluation, one need only specify only the time history of evolution (daily sequence) of ACPs throughout the year, and indicate whether it rains or not (anywhere within the basin) on a specific day. For hind casting, these data can be provided by an analysis of historical data and/or simulations provided by regional weather forecast models. For future projections, they can (in principle) be obtained from information provided by GCMs.

1.3. An alternative approach to evaluating potential impacts of climate change

Combined with GCM projections, the SRGP method therefore provides an intriguing alternative approach for evaluating the potential impacts of climate change on a basin. Since projected changes/variations in global climate can be expected to result in changes to global, regional and local patterns of atmospheric circulation – thereby resulting in changes to local intensities and spatial patterns of precipitation – the future projections provided by GCMs for various CO_2 emission scenarios can be used to obtain information regarding the anticipated time-evolution of

(a) The relative frequency of different kinds of atmospheric circulation patterns,
(b) The corresponding probability of rain,
(c) The mean areal temperature, and
(d) The relative change (from current period) in mean areal wet-day precipitation amount for each ACP type in each season.

This information can then be used to drive a hydrological model of the basin. In the case of catchment-scale lumped hydrological modeling, the information can be used directly, whereas for spatially distributed hydrological modeling the information can be used to generate high-resolution precipitation fields via SRGP method mentioned above.

Of course, application of this method requires us to make a number of important assumptions, including the following:

(AS1) Current GCMs are capable of providing sufficiently accurate simulations of atmospheric circulation patterns, probabilities of rain, and temperature under current conditions, and can predict their evolution under future potential emission scenarios.

(AS2) The GCMs can provide sufficiently accurate estimates of the evolution of relative changes in mean areal wet-day precipitation amount (changes from current day values) under future potential emission scenarios.

(AS3) Apart from the mean wet-day precipitation amounts, the mechanics of local spatial rainfall generation (properties of the spatial probability distributions and interactions with elevation) are not significantly altered.

It is possible to examine the validity of assumption AS1 for historical conditions, by evaluating the performance of GCMs against available data (Bronstert et al., 2007; Johnson and Sharma, 2009, 2011; Anagnostopoulos et al., 2010; Haberlandt et al., 2014); if the assumption is found to be defensible under current conditions, at least in a statistical way, we could (in principle) rely upon the GCMs to provide plausible information regarding their potential future evolution. Unfortunately, it is not practically possible to properly evaluate the validity of assumption AS2 since existing historical data records are insufficiently long to conduct a confident comparison of temporal trends, although some studies have at least analyzed the uncertainty of future GCMs projections (Déqué et al., 2007; Woldemeskel et al., 2012). We do know, however, that GCMs do not provide sufficiently accurate estimates of the actual values of precipitation (the estimates tend to be severely biased) although they do a fairly good job with respect to temperature (Johnson and Sharma, 2009; see also Section 2). Finally, it is impossible to establish the validity of assumption AS3 for reasons similar to AS2, and also because GCMs do not provide information at the scales necessary for local hydro-meteorological and water resources assessments.

2. Hydro-climatology of the Upper Guadiana Basin

The Upper Guadiana Basin (UGB) occupies a portion of the central Spanish Plateau (Fig. 1), and is characterized by relatively smooth changes in elevation ranging from 550 meters above sea - level (masl) at the basin outlet to more than 1000 masl at the northern and southern boundaries in the Sierra Altomira and Campos de Montiel respectively. Combined with lack of a well-defined drainage network and an abundance of large karstic formations, the smooth topography leads to high degree of connection between the surface and subsurface water. Around 250 km^2 of wetlands flourish in the basin due to regional groundwater discharge, including the natural wetlands of La Mancha Húmeda that has been declared a UNESCO Biosphere Reserve.

The basin experiences a mixed continental/semi-arid Mediterranean climate, with considerable spatio-temporal variability of precipitation due to both orographic effects (lapse rate of ~7.5 mm/km) and the climatic influences of the Atlantic Ocean and the Mediterranean Sea. Precipitation is measured daily at 49 gauge locations distributed evenly throughout the basin (Fig. 1), and records are available for the period January 1959 to December 2007; these values were aggregated to obtain mean areal values for the basin. Similarly, minimum, average and maximum daily temperature measurements are provided by the Spanish State Meteorological Agency (AEMET), and are available for the period January 1959 to December 2001.

These data will be represented using '*Climatology*' and '*ACPology*' plots. The '*Climatology*' plots display the annual pattern of monthly averages over the period 1960–1999, and are a conventional way of summarizing climate data for a region. In a similar manner, we propose the use of '*ACPology*' plots to group together the days associated with a particular atmospheric circulation pattern (ACP) type. Therefore, ACPology plots describe the climate in terms of the frequency of each ACP type and the mean weather associated with those atmospheric conditions.

The first step is to determine the ACP type for each day. For this study, we used an automated version of the Lamb Weather Type classification scheme (Jenkinson and Collison, 1977; Jones et al., 1993) based on the direction of surface wind and its vorticity in geostrophic units. Gridded values of Mean Sea Level Pressure (MSLP) were obtained at 16 points distributed as indicated in Fig. 1c (obtained from the gridded NCEP-NCAR re-analysis; Kalnay et al., 1996). Following previous applications of the automated version of the Lamb Weather Type classification scheme over the Iberian peninsula (Goodess and Palutikof, 1998; Goodess and Jones, 2002; Vicente-Serrano and López-Moreno, 2006; Sapriza Azuri, 2013; Lambán et al., 2015; Sapriza-Azuri et al., 2015) we obtain the 8 ACP types listed in Table 1. Types A1, A2 and A3 are directional patterns, A5, A6 and A7 are cyclonic (low

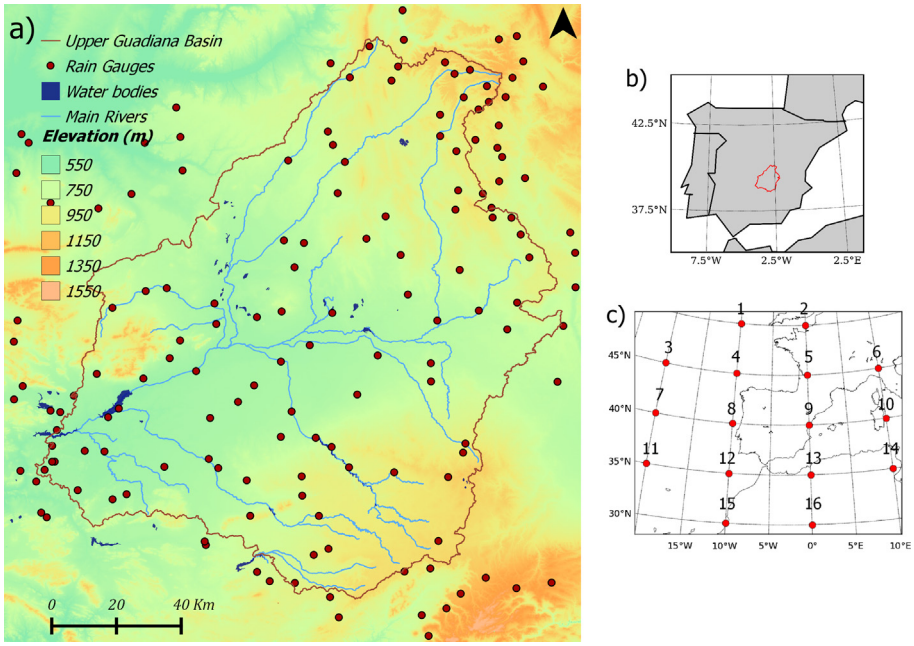

Fig. 1. (a) Map of the Upper Guadiana Basin, showing topographic elevation, main rivers and locations of rain gauges. (b) Location of the Upper Guadiana Basin in Spain. (c) Distribution of the 16 points used to compute the ACPs.

Table 1
List of ACP types.

ID	ACP type	Description
A1	Dir N-NW-W-SW	Northerly/NorthWesterly/Westerly/SouthWesterly directional types
A2	Dir E-NE	Easterly/NorthEasterly directional types
A3	Dir S-SE	Southerly/SouthEasterly directional types
A4	ACyclo	Anticyclonic and hybrid-anticyclonic
A5	Cyclo	Cyclonic
A6	Hyb Cyclo	Hybrid cyclonic
A7	Un/LFCyclo	Unclassified/ light flow cyclonic
A8	Un/LFACyclo	Unclassified/ light flow anticyclonic

pressure systems), and A4 & A8 are anti-cyclonic (high pressure systems). Fig. 2 shows the MSLP maps for the 8 ACP types obtained by averaging across the entire time period using the reanalysis data. To derive the ACPs from the GCMs (historical and future cases) we use the same discretization of grid cells, and use bilinear interpolation to match up with the same grid as the re-analysis data.

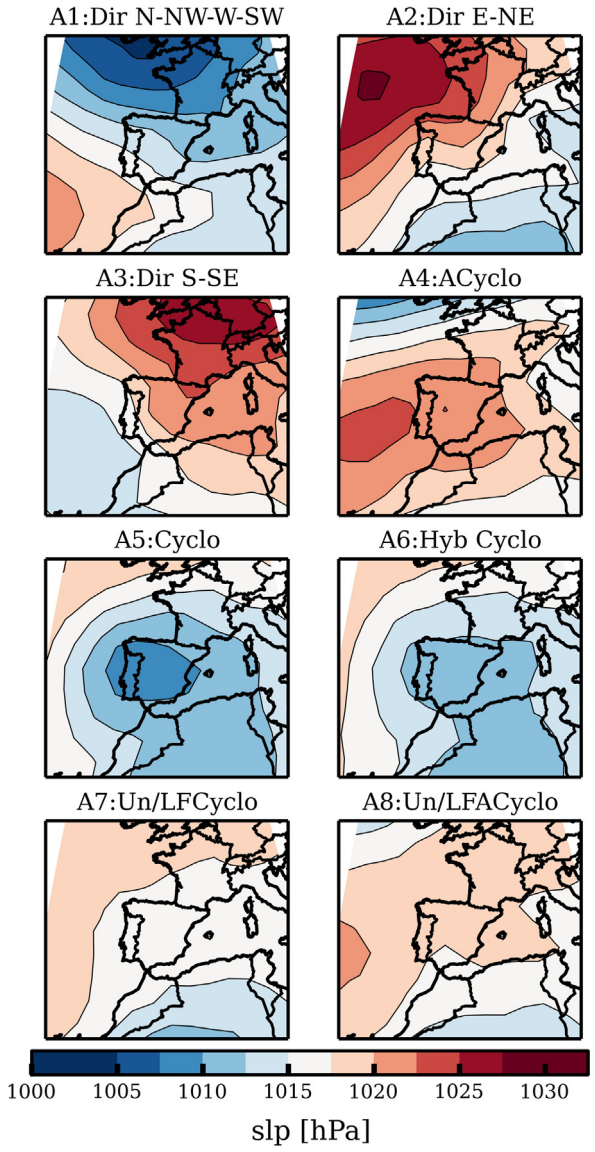

Fig. 2. Mean sea level pressure maps for the 8 ACP types using the re-analysis data NCEP/NCAR for the period 1960–1999.

'*Climatology*' plots of rainfall and temperature data are shown (as red lines) in the left column of Fig. 3, for the period 1960 to 1999. Here, a day is considered to be '*rainy*' if precipitation is recorded in at least one gauge in the basin, and the mean areal Wet Day Amount (*WDAm*) for each month is computed by summing the total (basin average) precipitation volume (*PVol*) for the month and dividing by the Number of Rainy Days (*NoRD*). The plots indicate that the precipitation (annual average ~475 mm/year) is characterized by strong seasonal variability, varying from 55 mm/-month in the winter (when the average temperature *TAvg* ~ 6 °C) to less than 10 mm/month during the hot summer months (July and August) when *TAvg* can exceed 25 °C. The low volume of summer precipitation is reflected in a low *NoRD* and *WDAm*.

The right column of Fig. 3 contains the corresponding 'ACPology' plots for the region. Of the 8 ACP types, A1, A4, A5 and A6 are particularly worth noting. The most frequent is A4 (130 days/year), which has the lowest Probability of Rain (*PoR* = 0.5) and lowest average Wet Day Amount (0.39 mm/day), therefore generating very little rain (only 25 mm/year). Being a high-pressure system, it is responsible for the characteristic '*sunny days*' that Spain is famous for. The second most frequent is A1 (65 days/year), a directional pattern (N/NW/W/SW) that brings moisture from the Atlantic Ocean and the Cantabric Sea, has a high *PoR* (0.85) and moderate *WDAm*, and therefore generates a very large amount of rain (152 mm/year). Finally, A5 and A6 are the '*wettest*' systems (being cyclonic, low-pressure), together accounting for 52 days/year, and having very high *PoR* (0.95 and 0.9 respectively); together they generate 198 mm/year (=112 + 86) of precipitation. The other four types (directional A2 and A3, and light-flow A7 and A8) occur during the remaining one-third of the year (118 days) but generate only about 21% (99 mm/year) of the rain. Note also that relatively cold temperatures generally accompany the wetter (A1, A5 and A6) systems, while the drier ones (A4, A2, A3, A7 and A8) are generally warmer.

Further details regarding the hydro-climatology of the various circulation patterns are shown in Fig. 4. The rows indicate different ACP types whereas each column illustrates a different hydroclimatic variable. The first column shows that A4 (anti-cyclonic) and A1 (directional N/NW/W/SW) display a clear seasonality in frequency of occurrence through the year (*NDays*), with marked declines in the summer, while A5, A6 and A3 are relatively flat. A2, A8 and A7 are more frequent in summer. The second column shows that in all cases, the Probability of Rain declines during the summer. Note also that the *PoRs* for A1, A5 and A6 are very close to 1.0 during the winter. The third column shows that the average Wet Day Amount can be quite variable throughout the year. Overall, it is clear that the local precipitation generation mechanism varies quite markedly with ACP type and time of year, and that higher temperatures (summer months) tend to be associated with lower Probabilities of Rain and smaller Wet Day Amounts. This is particularly true for the "rainmaking" circulation types, A1, A5 and A6.

3. Evaluation of global circulation model simulations

3.1. Qualitative evaluation

GCM simulations for the historical period (January 1959 to December 2005) are available from Phase 5 of the Coupled Model Intercomparison Project (CMIP5 http://cmip-pcmdi.llnl.gov/cmip5/) (Taylor et al., 2011). Data are available for the 20 models listed in Table 2. Each of these models is represented in Figs. 3 and 4 by a gray line. The GCM ensemble model, estimated as the median, is plotted as a black line. Spatial patterns of MSLP by

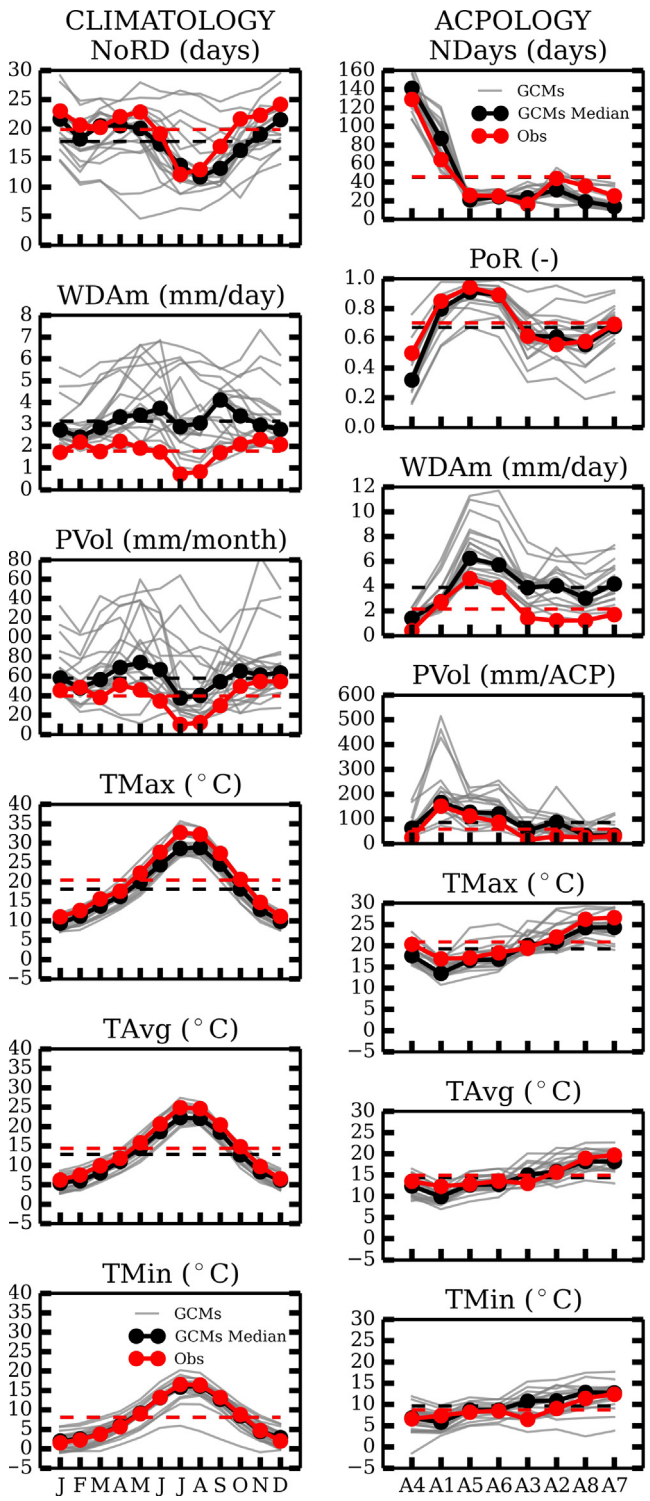

Fig. 3. Hydro-Climatology (left column) and Hydro-ACPology (right column) of the Upper Guadiana Basin for the 40-year period 1960–1999. The red line indicates observed values (dashed is the overall mean). The GCMs, which will be addressed in Section 3, are represented by gray lines and their median by black line (dashed is the overall median). The variables shown are *NDay* = Number of ACP Days (days/year); *NoRD* = Number of Rainy Days (days/month, or days/ACP per year); *PoR* = Probability of Rain (NoRD/NDay); *WDAm* = Wet-Day Amount (mm/day); *PVol* = Precipitation Volume (mm/month or mm/ACP per year); *TMax* = Maximum Daily Temperature (°C); *TMin* = Minimum Daily Temperature (°C); *TAvg* = Mean Daily Temperature (°C). (For interpretation of the references to color in this figure legend, the reader is referred to the web version of this article.)

ACP of reanalysis-based (first column in both figures) and GCMs-based are shown in Figs. 5a and 5b.

The left column of Fig. 3 shows that all of the GCMs tend to do a very good job of reproducing the Climatological '*Level*' and '*Pattern*' of temperature, although with a slight negative bias. The only notable outlier is model *InmCM4* (GCM-11), which has a very severe cold bias for Daily Minimum Temperature (*TMin*). Similarly, 13 of 20 of the GCMs track the pattern and level of the Number of Rainy Days (*NoRD*) reasonably well, although with a slight tendency to underestimation (~2 days/month on average).

Meanwhile, as is reported by others (Dai, 2006; Kundzewicz et al., 2008; Anagnostopoulos et al., 2010), most of the GCMs provide poor prediction of the climatological level and pattern of Wet Day Amount (*WDAm*), and hence Precipitation Volume (*PVol*). Note that many of the GCMs do not even reproduce the Summer decline in Wet Day Amount, and some of them actually overestimate the *WDAm* level by as much as 300%.

In contrast, the right column of Fig. 3 shows that all of the models tend to reproduce the ACPology patterns quite well. In fact, the frequency distribution of ACPs (Number of ACP days per years) is reproduced very closely. Similarly, the Number of Rainy Days per ACP (and hence the *PoR*) is also reproduced very well, with some disagreement for the fine weather A4 (anti-cyclonic) system. Further, the ACPology of temperature is well represented (although again GCM-11 shows a cold bias for *TMin*).

Meanwhile, although the magnitude (level) of *WDAm* (and hence *PVol*) for all ACPs tends to show a strong positive bias, the '*pattern*' (relative values across the ACPs) is quite well reproduced.

To analyze the evolution of ACPs frequency during the historical period, we compare in Fig. 6 the annual frequency of ACPs over three 15-year windows (1961–1975, 1976–1990 and 1991–2005). Results are similar for the three periods and to those of the entire historical period (Fig. 3 top plot of the right column). This finding is relevant because it supports our first assumption (AS1 in the Introduction) that GCMs are quite accurate in reproducing ACP frequencies. In fact, given the significant reduction in rainfall over the Guadiana Basin during the historical period studied (Sapriza Azuri, 2013), this finding suggests that it is possible that ACP frequencies may also be reproduced skillfully by GCMs under conditions of changing climate.

The GCM simulations of MLSP spatial patterns (Figs. 5a and 5b), all tend to represent the A1 (directional N/NW/W/SW) and A4 (anti-cyclonic) ACPs well, but provide poorer representations for the A3 (directional E-NE), A5 (Cyclonic) and A6 (Hybrid Cyclonic) ACPs. Overall, only three of the GCMs (GCM-2, GCM-14 and GCM-15) reproduce the spatial patterns of all the ACPs reasonably well, and although GCM-18 is able to reproduce the spatial pattern, it displays a clear negative bias in the magnitude of simulated MSLP.

Overall, these plots indicate that while GCMs differ widely in terms of how well they reproduce the generation of rainfall amount, they actually tend to provide quite good simulations (in terms of climatology and ACPology) for Temperature, frequency distribution, spatial pattern of ACPs, and Probability of Rain. In terms of the stated goals of this study, this is good news as it suggests the possibility of being able to rely upon future projections of atmospheric circulation patterns and their corresponding probabilities of rain for water resources assessments. However, it is clear that we cannot rely upon the GCMs to accurately simulate the magnitudes and climatological patterns of Wet Day Amounts.

It would be useful, therefore, to evaluate quantitatively whether any of the 20 models is actually better (than the others) in terms of its simulation of the hydro-climatology of the Upper Guadiana Basin.

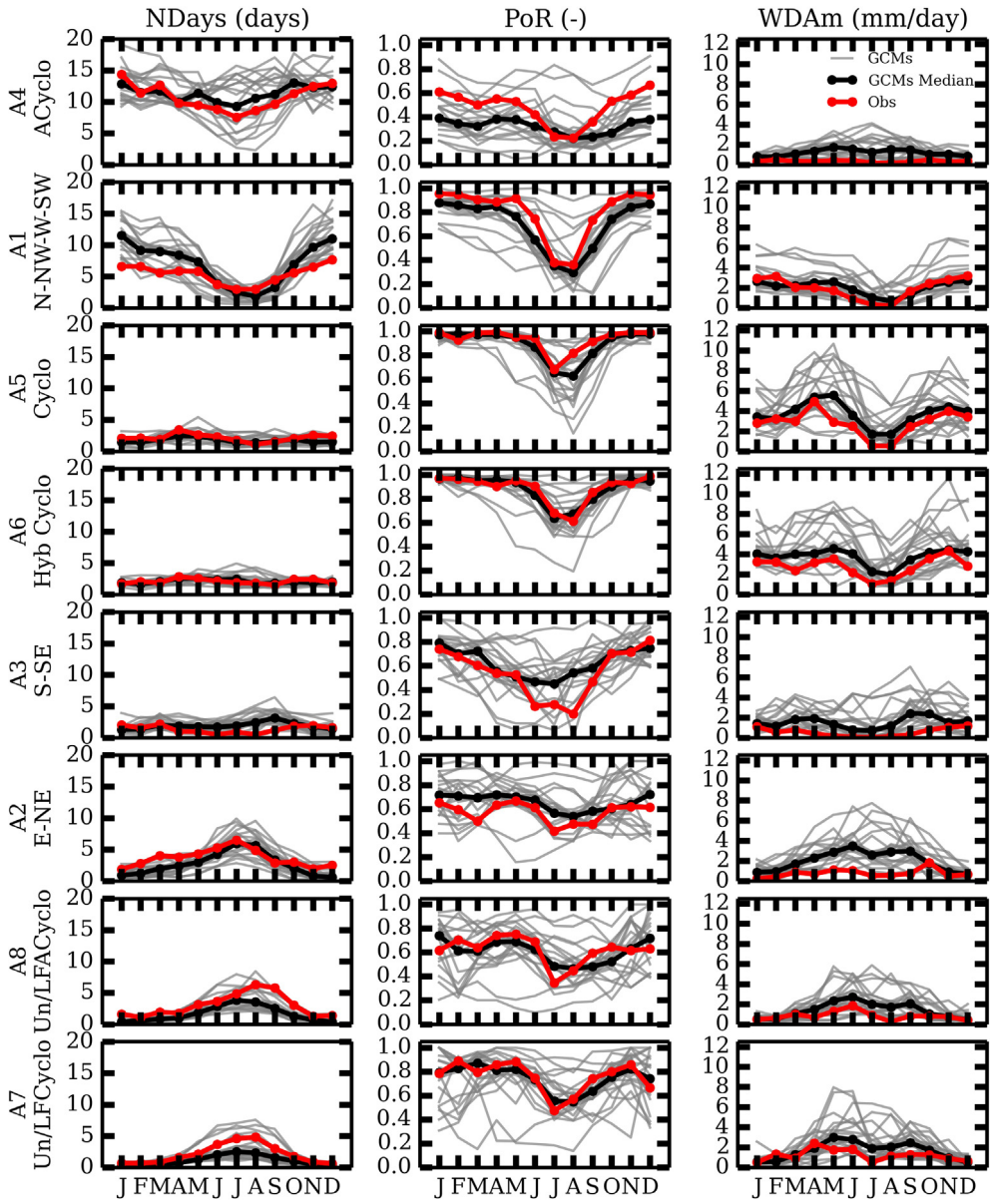

Fig. 4. Hydro-Climatology of each ACP. Red lines indicate observed values, each gray line is for a different GCM, and the black line indicates the median of the set of GCMs. For each ACP, the first column shows the Number of ACP Days per month, the second column shows the Probability of Rain per month, and the third column shows the mean daily Wet-Day Amount. (For interpretation of the references to color in this figure legend, the reader is referred to the web version of this article.)

3.2. Quantitative evaluation

To perform a more quantitative evaluation of GCM performance, we compute two measures of Climatological similarity for each variable – {*RL* = *Relative Level*} and {*SC* = *Shape Correlation*}. The measure *RL* simply reports the mean value of the GCM climatology divided by the mean value of the observed climatology (for a given variable) and so varies on [0 ∞]; its value equals 1.0 if the overall level (i.e. monthly mean) is perfectly matched, and is larger than 1.0 if the GCM overestimates observations. Similarly, the measure *SC* reports the corresponding simple linear correlation between the GCM climatology values and the observed values, and so varies on [−1.0 1.0]; its value equals +1.0 if the shape of the monthly climatology is perfectly reproduced. If both *RL* = 1 and *SC* = 1, then the GCM reproduction of climatology (Fig. 3 left column) can be considered "*perfect*" (in an annual average sense). Similarly, *RL* and *SC* can be computed for the ACPologies (Fig. 3 right column) and the ACP-climatologies of each variable (Fig. 4). These results are plotted in Figs. 7 and 8, it should be understood that our findings are not meant to indicate that any particular GCM is "*good*" or "*bad*" in any overall sense; our methodology here simply helps to identify which GCMs do a good job for any particular region – in our case the Upper Guadiana Basin.

The first and third subplot of Fig. 7 show model performances in terms of *RL* and *SC* of climatology. As mentioned earlier, all of the models perform well on temperature, with shape correlations close to 1.0 and relative levels in the range [0.5 1.5]. However, reproduction of *TMax* and *TAvg* is much better than for *TMin*, where the model spread is much larger. Further, 11 out of 20 models show good performance on Number of Rainy Days (*NoRD*). Shape correlations are within the range [0.5 1.0] and within [0.75 1.0] for relative level.

The second and fourth subplot of Fig. 7 shows model performance in terms of *RL* and *SC* of ACPology. Here we find that all of

Table 2
List of GCMs.

ID	GCM
1	CanESM2
2	CnrmCM5
3	CsiroMK36
4	HadCM3
5	IpslCM5A-LR
6	IpslCM5A-MR
7	MirocESM
8	MirocESM-CHEM
9	GfdlESM-2G
10	GfdlESM-2M
11	InmCM4
12	MriCGM3
13	NorESM1
14	HadGEM2-CC
15	HadGEM2-ES
16	GissE2R
17	ACCESS
18	EC-EARTH
19	MPI-ESM-LR
20	MPI-ESM-MR

the shape correlations are generally high with the exception of *TMin* for models 4 and 11 (*HadCm3* and *InmCM4*), and in general the relative levels are within the [0.5 1.5] range for the temperatures and *PoR*.

If we reject the following 14 models for the reasons listed below, we are left with only the six GCMs indicated by the light blue markers.

(a) Model 11 for its cold *TMin* bias in both climatology and ACPology (*RL* < 0.5).
(b) Models 2, 5, 12, 13, 14, 16 and 17 for *NoRD* climatology *SC* < 0.5.
(c) Model 6 for *NoRD* climatology *RL* < 0.5.
(d) Models 7, 8, 9 and 10 for *WDAm* climatology *SC* < 0.
(e) Model 4 for its cold *TMin* bias in ACPology (*RL* < 0.5).

The remaining models correspond to {1 = *CanESM2*, 3 = *CsiroMK36*, 15 = *HadGEM2-ES*, 18 = *EC-EARTH*, 19 = *MPI-ESM-LR*, and 20 = *MPI-ESM-MR*}. With the exception of rainfall amounts (*WDAm* and *PVol*), these models can be said to provide "*excellent*" performance in terms of *NoRD*, *TMax* and *TAvg* climatology and *PoR*, *TMax* and *TAvg* ACPology, and relatively "*good*" performance in terms of *TMin*. Further, although the *WDAm* values (and hence *PVol*) tend to be high, and therefore in need of bias correction, the climatology shape correlations are all positive and the ACPology shape correlations are all above 0.7.

Further details about the climatological performance of each model for individual ACPs can be seen in Fig. 8. Each column corresponds to one of the eight ACPs and the six subplots correspond to Number of ACP Days per month (*NDay*), *PoR* and *WDAm RL and SC respectively*. The selected "*good*" models do a remarkable job of reproducing the climatological *SC's* of *NDay*, and *PoR* for A1 (directional N/NW/W/SW) that brings moisture from the Atlantic Ocean and Cantabric Sea, but with a tendency to have too many days of this type, and with a marked (50%) dry bias. In contrast the reproduction of climatological *SC's* for the cyclonic A5 and A6 types is weaker (although *RL* values are relatively close to 1.0), and with a substantial wet bias. Interestingly, only 2 of the "*good*" models (15 = *HadGEM2-ES* and 18 = *EC-EARTH*) do a decent job for the

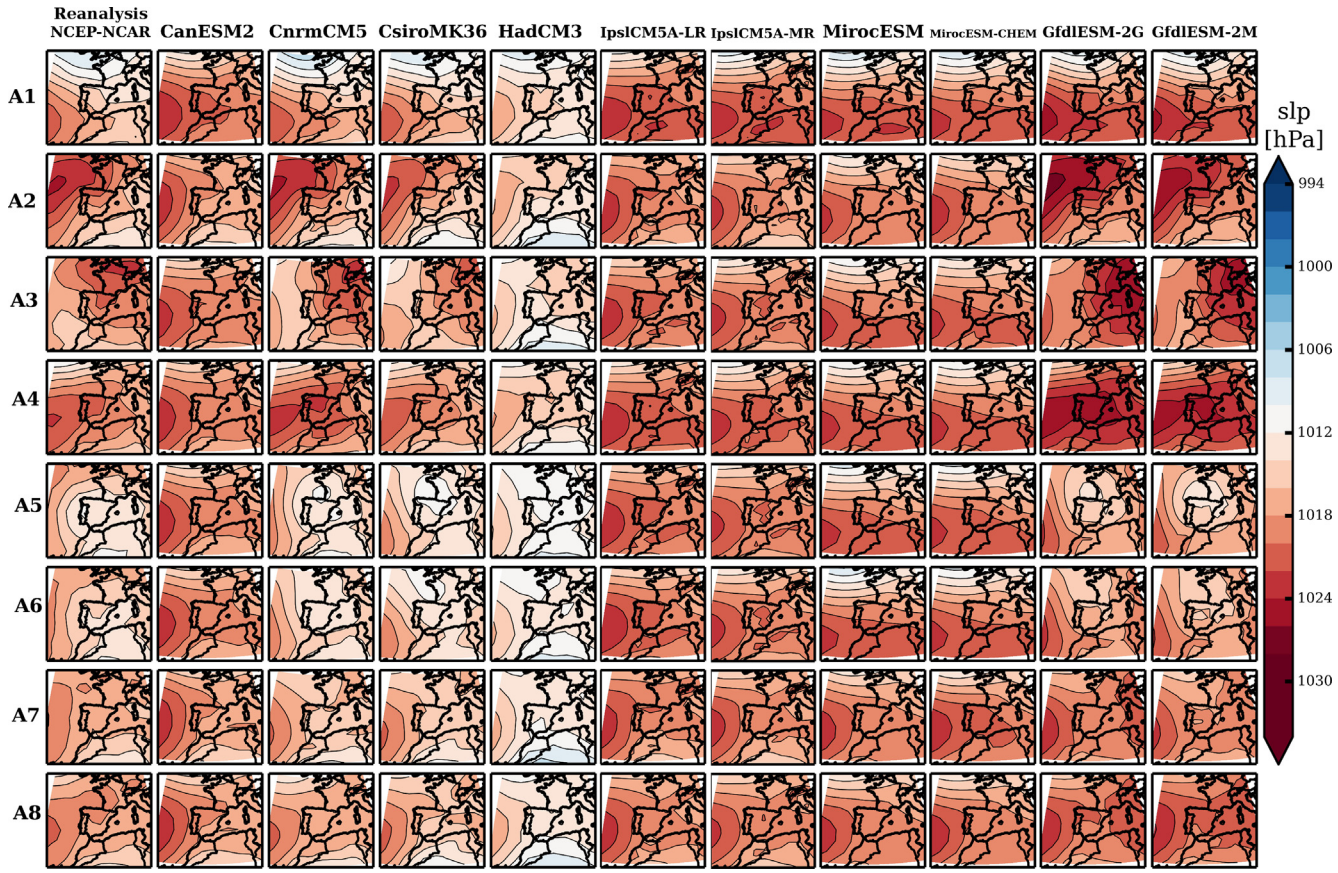

Fig. 5a. Comparison of time averaged mean sea level pressure maps for the 8 ACP using the re-analysis data (first column) and GCM-based (GCM1 to GCM10).

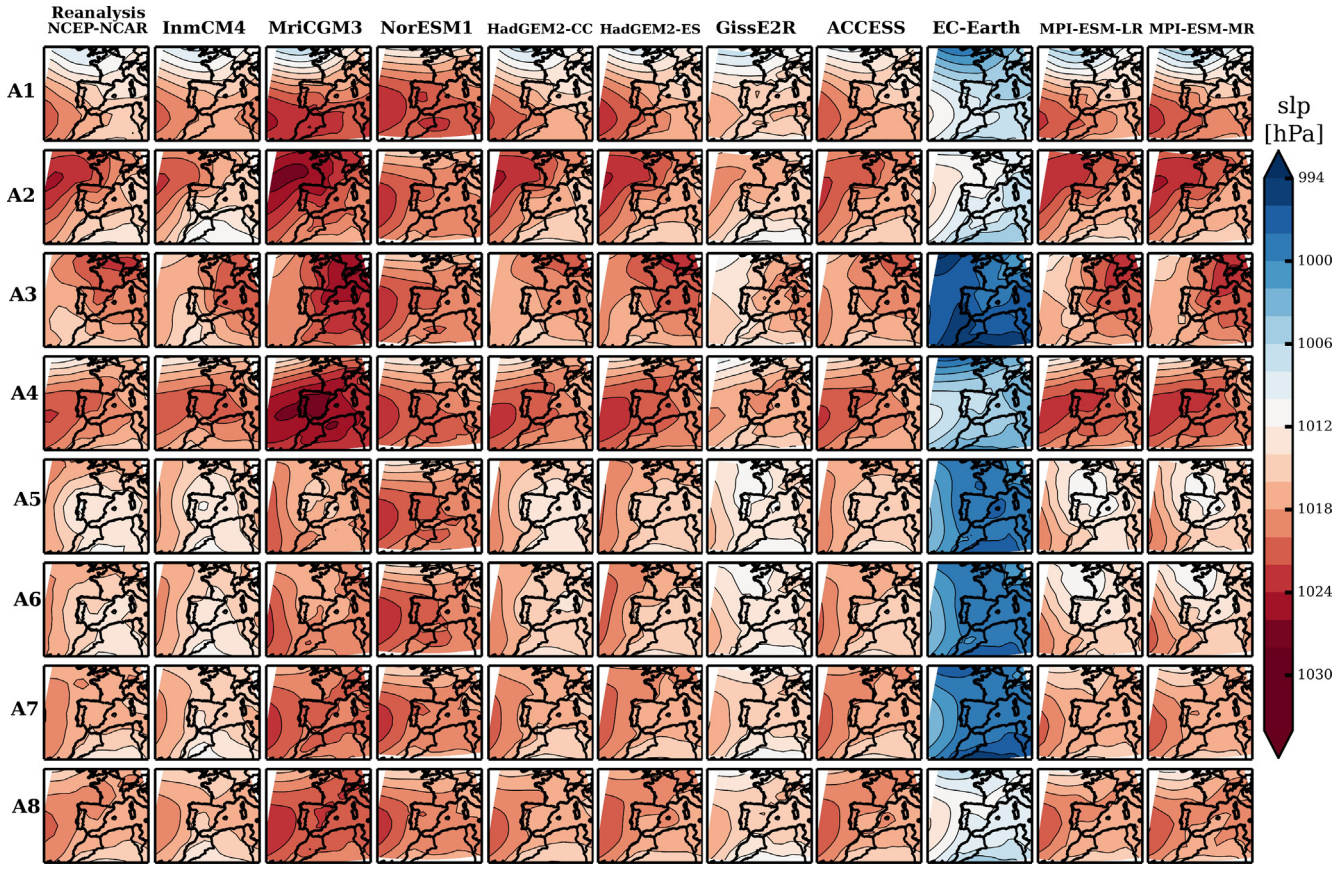

Fig. 5b. Comparison of time averaged mean sea level pressure maps for the 8 ACP using the re-analysis data (first column) and GCM-based (GCM11 to GCM20).

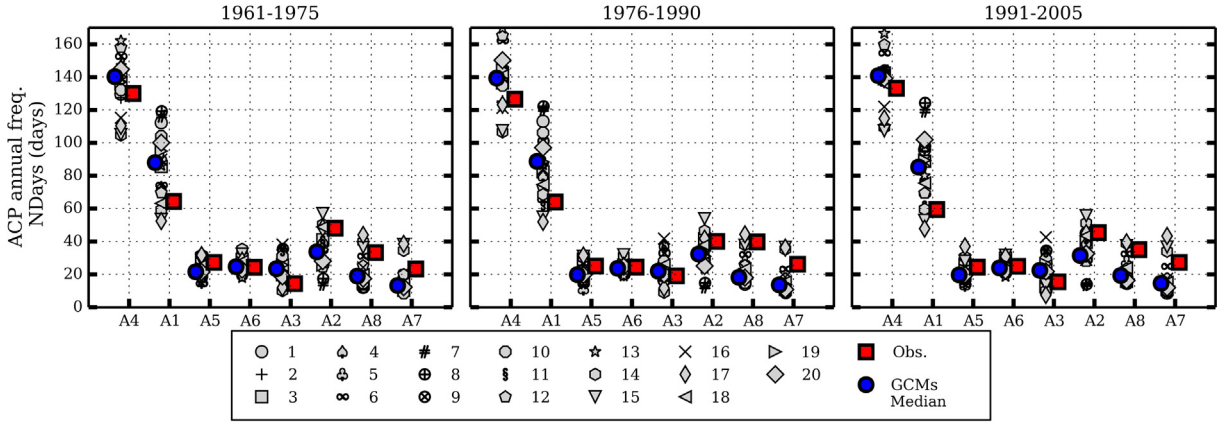

Fig. 6. Mean annual frequency of number of ACP over three window of 15-year historical period (left panel 1961–1975, center panel 1976–1990 and right panel 1991–2005). Markers numbers correspond to GCMs numbers in Table 2, the red square and the blue circle corresponds to observations (re-analysis based) and GCMs median respectively. (For interpretation of the references to color in this figure legend, the reader is referred to the web version of this article.)

anti-cyclonic A4 high-pressure system, and all models have a very severe dry bias. The ACP type for which the models disagree the most is the A3 (directional S/SE) system, and the performance on the remaining types (A2, A7 and A8) is moderately good, though somewhat varied.

To evaluate the abilities of the GCMs to reproduce the spatial pattern of MSLP by ACP we compute two statistics: the root mean square error (RMSE) at the grid points of MSLP (averaged over all days belonging to each ACP in every model) using the reanalysis data as true and the pattern correlation (PC) computed as the correlation coefficient of the same data. Fig. 9 displays the results in matrix form. In general, 4 of the 6 GCMs selected above as "good" models perform well here, with a low RMSE < 20 Pa and greater than 0.5 PC. GCM-18 (EC-EARTH) reproduces the reanalysis patterns (mean PC for the 8 ACP is 0.87), but scores the worst of all GCMs in terms of RMSE (due mainly to the fact – see Fig. 5b – that MSLP is severely underestimated). GCM-1 (CanESM2) fails to reproduce the spatial pattern of A3 (PC = −0.42), A5 (−0.10) and A6 (0.23). The GCMs that best reproduce the spatial patterns (mean RMSE over all ACPs < 10 Pa and PC > 0.9) are GCM-14 (HadGEM2-CC), GCM-15 (HadGEM2-ES), GCM-17(ACCESS), and GCM-2 (CnrmCM5).

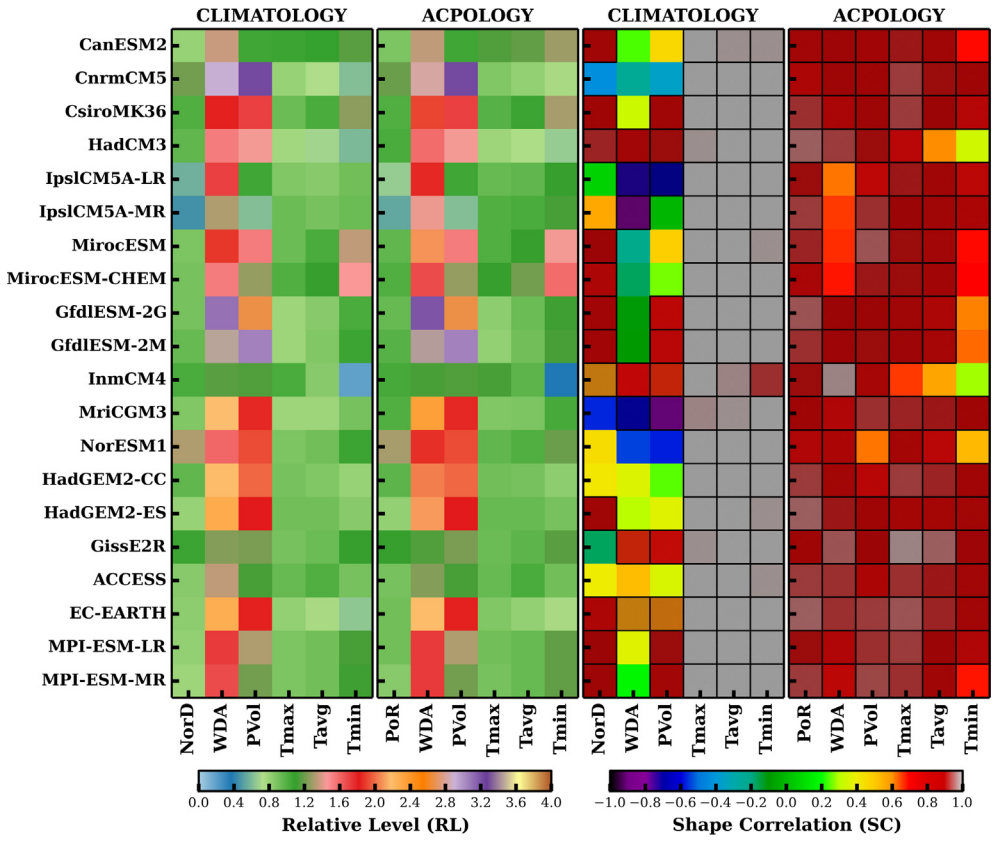

Fig. 7. Quantitative evaluations of the Hydro-Climatology and Hydro-ACPology of each GCM (rows), against observed values, for the historical 40-year period 1960–1999. The left subplots (RL = Relative Level) measures the accuracy in the mean whereas the two subplots to the right (SC = Shape Correlation) measures the accuracy in the shape of the distribution of the variable as shown in Fig. 2. The Hatched lines represent *p*-values <0.05 for SC. Variable names are as indicated in Fig. 2.

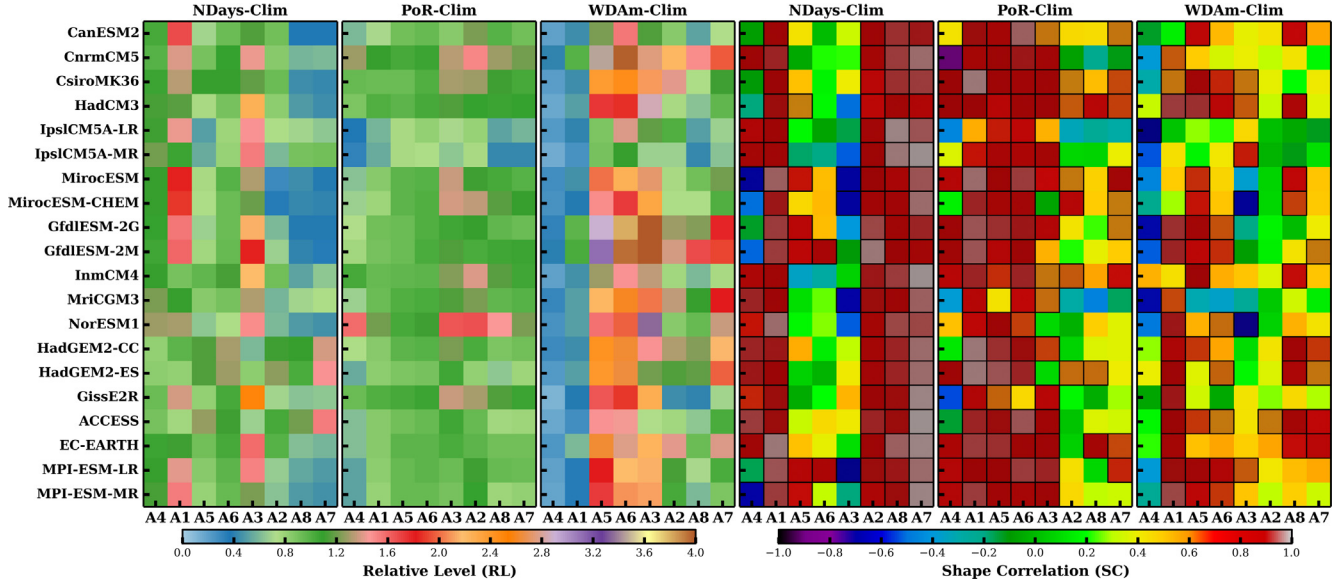

Fig. 8. Quantitative evaluation of the Hydro-Climatology by ACP type of each GCM (markers), against observed values, for the historical 40-year period 1960–1999 (SC = Shape Correlation and RL = Relative Level). Hatched lines represent *p*-values <0.05 for SC. Variable names are as indicated in Fig. 7.

3.3. Summary of GCM evaluation

In conclusion, our quantitative evaluation of GCM performance indicates that four of the 20 GCMs participating in the IPCC Assessment can be considered to provide reasonably good simulations of the hydro-climatology, ACP-hydro-climatologies and the ACP-spatial patterns (RMSE and PC) of the Upper Guadiana Basin (with the exception of Wet Day Amounts associated with each atmospheric circulation pattern). Therefore, to carry out an assessment of the potential impacts of climate change on this basin, we focus on the four selected models and use them to provide time series of daily ACP type, occurrence (or not) of rain, and temperature for this

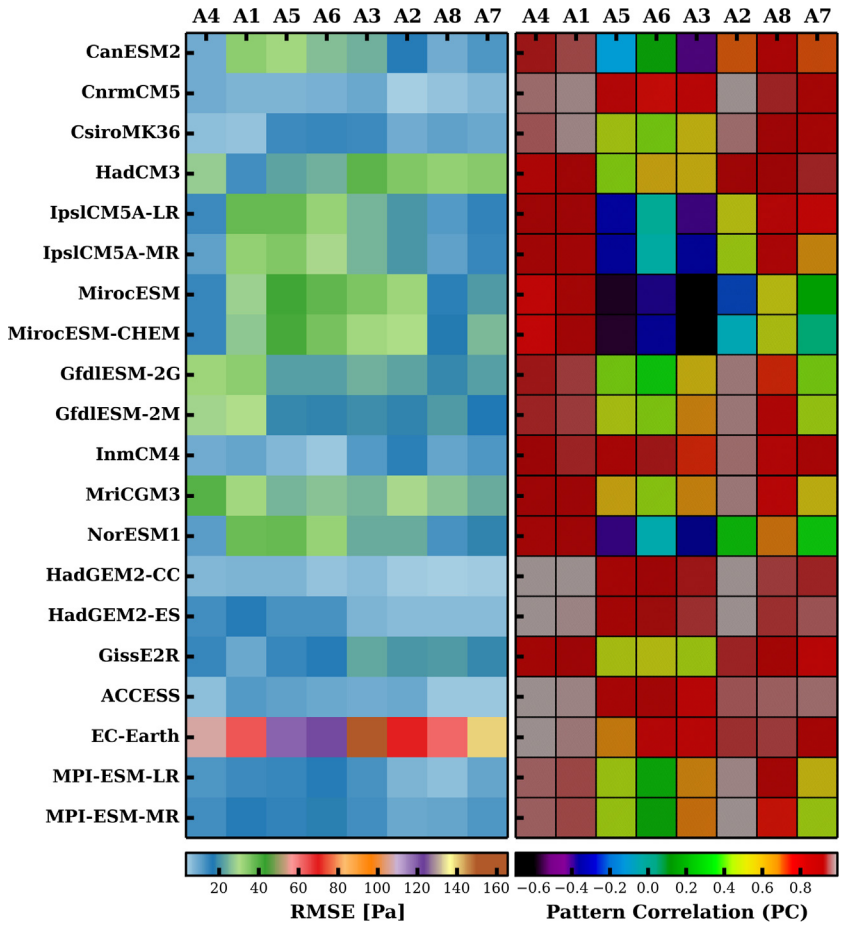

Fig. 9. Quantitative spatial pattern evaluation of the MSLP maps for the 8 ACP comparing observation (re-analysis based) and GCM-based for the historical 40-year period 1960–1999. Left panel shows the spatial Root Mean Square Error (RMSE) and right panel Pattern Correlation computed as Pearson correlation coefficient. Hatched lines represent p-values <0.05 for pattern correlation.

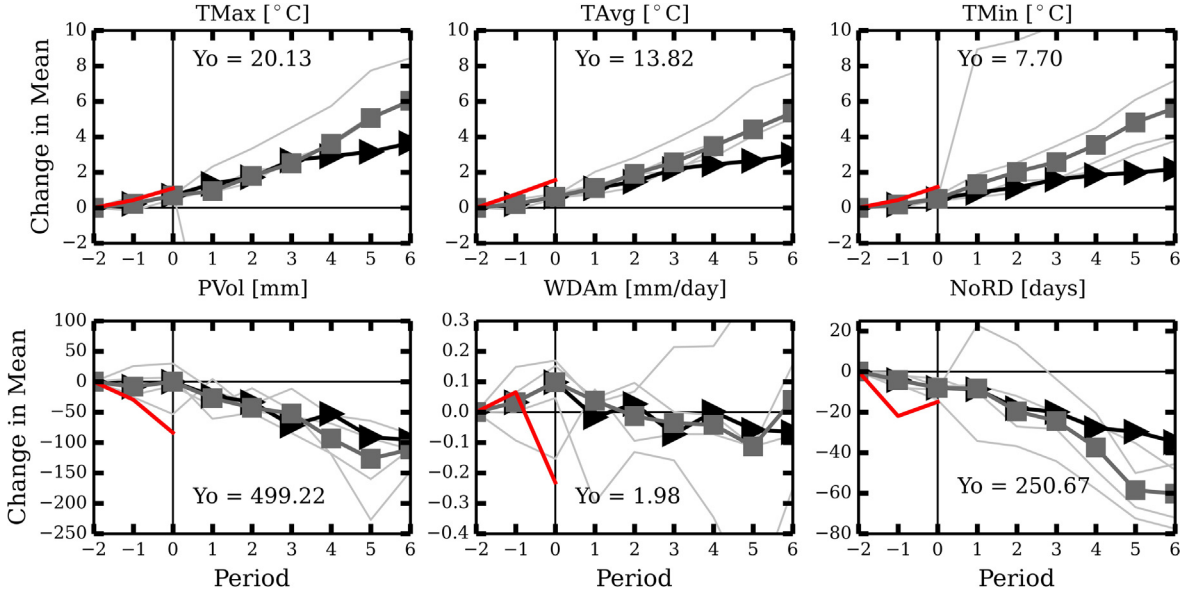

Fig. 10. Analysis of Projected Trends due to increases in radiative forcing. Each line indicates the trend of mean annual values computed on the 15-year intervals (−2 = 1961–1975); (−1 = 1976–1990); (0 = 1991–2005); (1 = 2006–2020); (2 = 2021–2035); (3 = 2036–2050); (4 = 2051–2065); (5 = 2066–2080) and (6 = 2081–2095). The light gray lines indicates the *RCP 8.5* scenario-projection by the four 'good' models selected for the Upper Guadiana Basin {*CsiroMK36, HadGEM2-ES, MPI-ESM-LR, and MPI-ESM-MRI*}. The heavy gray line indicates the median of the *RCP 8.5* projections, the heavy black line indicates the median of the *RCP 4.5* projection, and the red line indicates the observed values. (For interpretation of the references to color in this figure legend, the reader is referred to the web version of this article.)

region. Further, to generate simulations of precipitation amount, we apply appropriate bias corrections to the climatological patterns of Wet day Amount associated with each ACP type (see Fig. 4).

The thresholds selected to retain a GCM for future climate projections over our study region are SC > 0.5 and 1.5 > RL > 0.5. As for the spatial pattern, we have used RMSE < 20 Pa and PC > 0.5. However, it seems plausible that actual thresholds may need to be site dependent, reflecting the facts of model uncertainty and variability among models.

4. Climate change projections for the upper guadiana basin

In this section, we examine the climate change projections provided by the four "*good*" models identified in Section 3, with a view to understanding how the hydro-climatology of the Upper Guadiana Basin might be expected to change over the next 100 years. Rather than use the A1-A2-B1-B2 emission scenarios presented in 'The Special Report on Emissions Scenarios' (SRES; IPCC, 2000), which were the basis for the *3rd and 4th IPCC Assessment Reports (2001, 2007)*, we follow the new '*Representative Concentration Pathways*' (RCP) approach developed for the 5th IPCC Assessment Report (http://www.wmo.int/pages/themes/climate/emission_scenarios.php). Note that we have not applied any kind of correction for the future MSLPs need to calculate the future ACPs.

4.1. Selection of climate change scenarios

For this analysis we selected RCP 4.5, which represents a '*Medium–Low Representative Concentration Pathway*', and RCP 8.5, which represents a more severe '*Rising Radiative Forcing Pathway*' (Moss et al., 2010; van Vuuren et al., 2011). Therefore, these two scenarios represent jointly a plausible range of potential emission scenarios for the future, whereas the impacts determined under RCP 8.5 might be considered to represent a sort of upper limit. The projections provided by the 20 participating GCMs for the period 2006–2100 (see Table 2) can be downloaded from CMIP5 project http://cmip-pcmdi.llnl.gov/cmip5/. Note that while complete data were not available at the time of this analysis for GCM-4 (*HadCM3*) and GCM-16 (*GissE2R*), these two GCMs do not belong to the set of models selected as providing "*good*" simulations for the Upper Guadiana Basin.

4.2. Analysis of future trends

Figs. 10–12 present an analysis of future trends projected by the four selected GCMs for the RCP 4.5 and RCP 8.5 scenarios. To construct these plots, the 135-year period from 1961 to 2095 was subdivided into nine periods each being 15 years in length, thereby constituting three historical periods (1961–1975, 1976–1990 and 1991–2005) and six future periods (2006–2020, 2021–2035, 2036–2050, 2051–2065, 2066–2080 and 2081–2095).

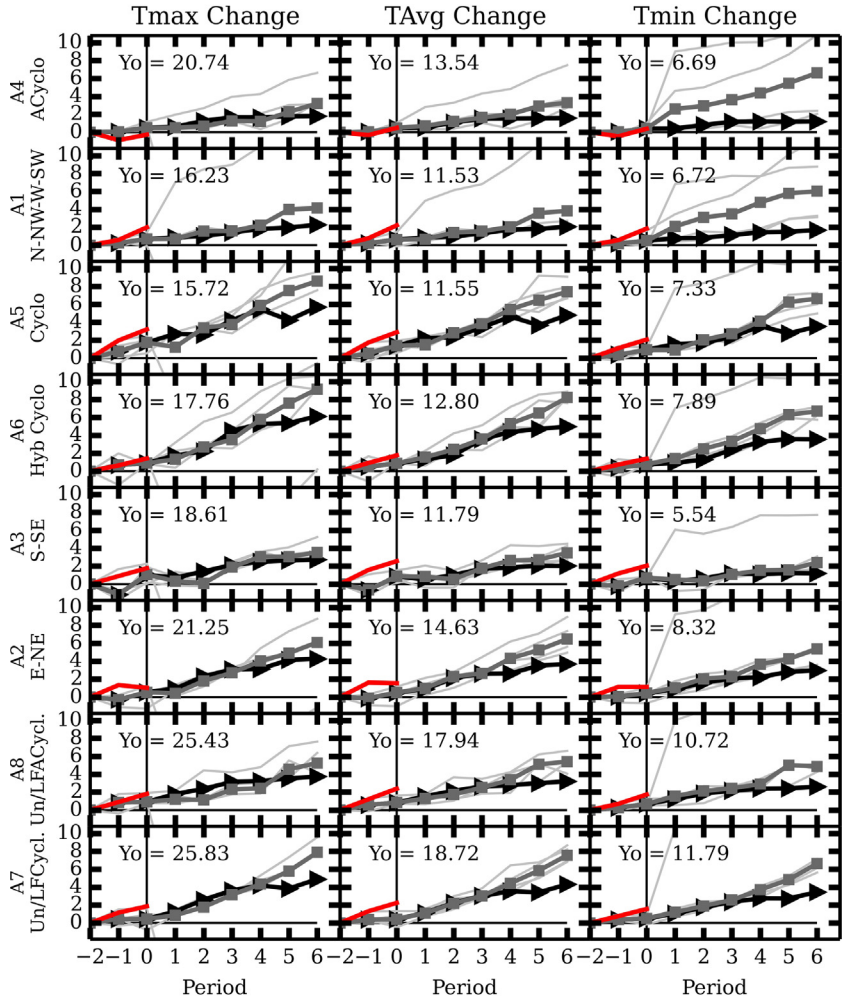

Fig. 11. Analysis of Projected Trends by ACP. Columns correspond to the 8 ACP types. The columns correspond to *TMAx*, *TAvg* and *TMin*. Other information is as provided for Fig. 10.

In general, our analysis of the results shows that the bias in GCM simulations of precipitation can be corrected using a multiplicative factor. This finding is consistent with the fact that the pdf for precipitation tends to follow a log-normal or gamma distribution. By adjusting the mean by a multiplicative factor, we correct both the mean and the variance, in contrast with an additive correction that would simply move the mean of the pdf without affecting other moments of the distribution. So, for each variable, we first compute the period mean (observation and GCM), and then perform the following adjustment to remove the bias:

$$Adjusted\ GCM\ \ value = GCM\ \ value \times \frac{Observed\ Value\ for\ 1961{-}1975}{GCM\ Value\ for\ 1961{-}1975}$$

We then plot the difference between the adjusted value for any period and the corresponding value for the first period (1961–1975); as indicated earlier, this adjustment can be fairly large for *WDAm* and *PVol*. Note that, given the nature of the adjustment, these plots can be viewed as projected changes from the 1961–1975 baseline value.

In each figure, the four light gray lines represent the projections provided by each of the four selected GCMs for the RCP 8.5 scenario (to avoid confusion the RCP 4.5 lines for the individual models are not included), the heavy gray line shows the median of these RCP 8.5 projections, and the black line shows the median of the RCP 4.5 projections. The *x*-axis labels {−2, −1, 0} represent the three historical periods and the labels {1 thru 6} represent the future periods. Since we are showing changes (differences) from the first period, the plots also indicate the corresponding baseline values as {*Yo* = . . .}.

The results in Fig. 10 show the expected progressive rise in temperatures. Note that the two scenarios only begin to diverge around 2036–2050, when the changes tend to accelerate for RCP 8.5 and decelerate for RCP 4.5. Overall, the plots indicate that daily mean temperatures (*TAvg*) can be expected to increase by 3.3–5.8 °C by the end of the 21st century, with maximum daily temperatures rising somewhat more quickly. Note however, that the model projections do not rise as quickly as the observations during the historical period, hinting at the fact that the GCMs may actually be underestimating temperature rises.

The Number of Rainy Days is projected to decline (on average) by 34–63 days per year and the Wet Day Amount by 0.13–0.25 mm/day (3.0–7.5 mm/month; 7–13%). The consequent

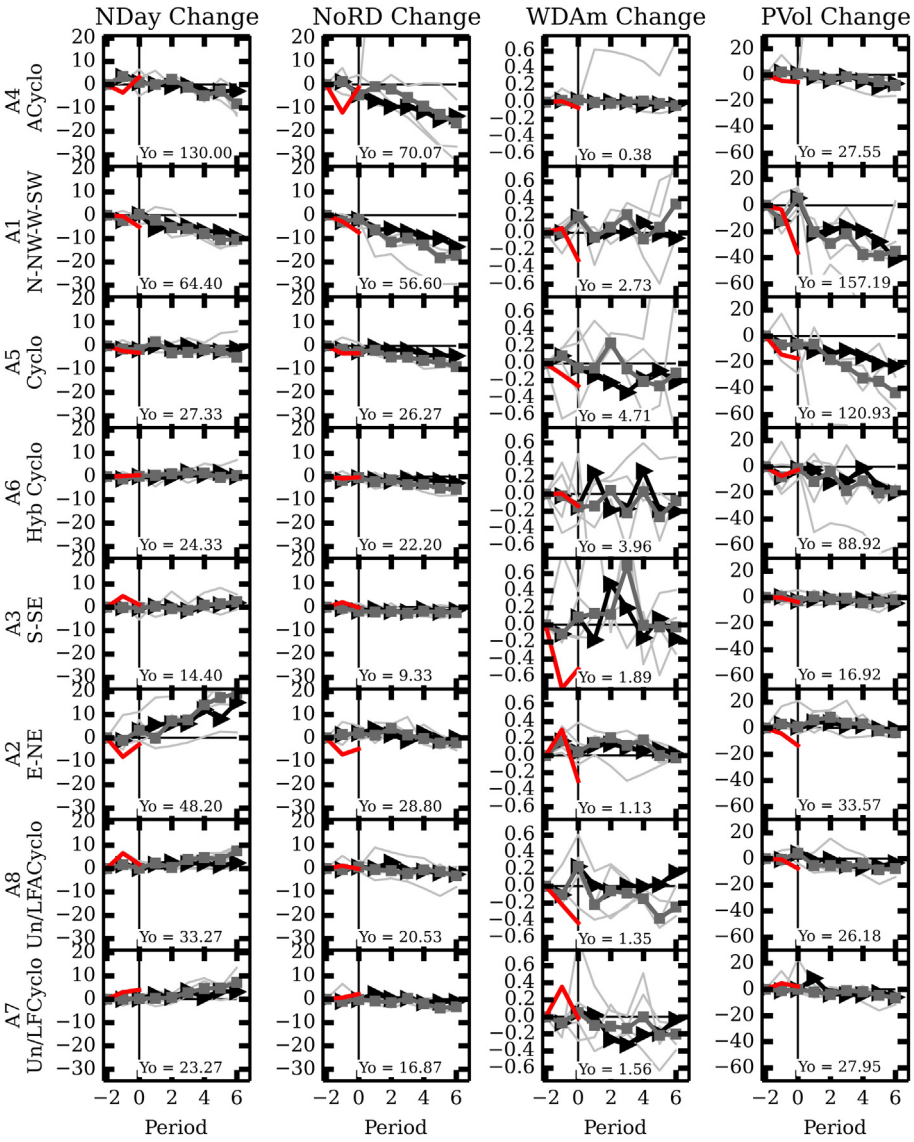

Fig. 12. Analysis of Projected Trends by ACP. Rows correspond to the 8 ACP types. The columns correspond to the Number of ACP Days (*NDay*), Number of Rainy Days (*NoRD*), Wet Day Amount (*WDAm*) and mean annual Precipitation Volume (*PVol*). Other information is as provided for Fig. 10.

reduction in precipitation volume is projected at 100–160 mm/year, which corresponds to a 20–30% decrease in mean annual precipitation. However, note again that observed historical *PVol* declined faster than the model projections, hinting that the GCM projections of precipitation decline may also be underestimates. Clearly, the amount of model ensemble spread for *WDAm* (less so for *NoRD*), and the lack of agreement between the ensemble mean and historical observations, indicates considerable uncertainty in the future magnitude of precipitation. For example, one of the models (*MPI-ESM-MR*) actually projects a potential '*increase*' in Wet day Amount.

The results in Figs. 11 and 12 show the details broken out by each of the 8 ACP types. Fig. 11 shows that the temperature increases, and also the differences between responses to the two warming scenarios, are larger for some ACPs than for others. For example the scenario differences are relatively small for A3 (directional S/SE), which brings winds from over the Mediterranean Sea and Africa. In contrast, the scenario differences for A5 and A6 (cyclonic, low pressure) are much larger, and the projected increase in *TMax* is as high as 9 °C (above a baseline of 15.7 °C). Note that the warmest ACP is A7 (low-flow) with *TMax* reaching 34 °C.

Fig. 12 shows the corresponding changes in Number of ACP Days (*NDay*; first column row), Number of Rainy Days (*NoRD*; second column), Wet Day Amount (*WDAm*; third column) and mean annual Precipitation Volume (*PVol*; last column). The most striking result shown here is that the models indicate that projected increases in radiative forcing (and hence temperature) will only impact some of the properties of some of the ACPs in a considerable way. For example, the projections indicate that the relative frequencies of the ACPs are only moderately affected, with A1 (directional N/NW/W/SW) showing the strongest decline (10 days

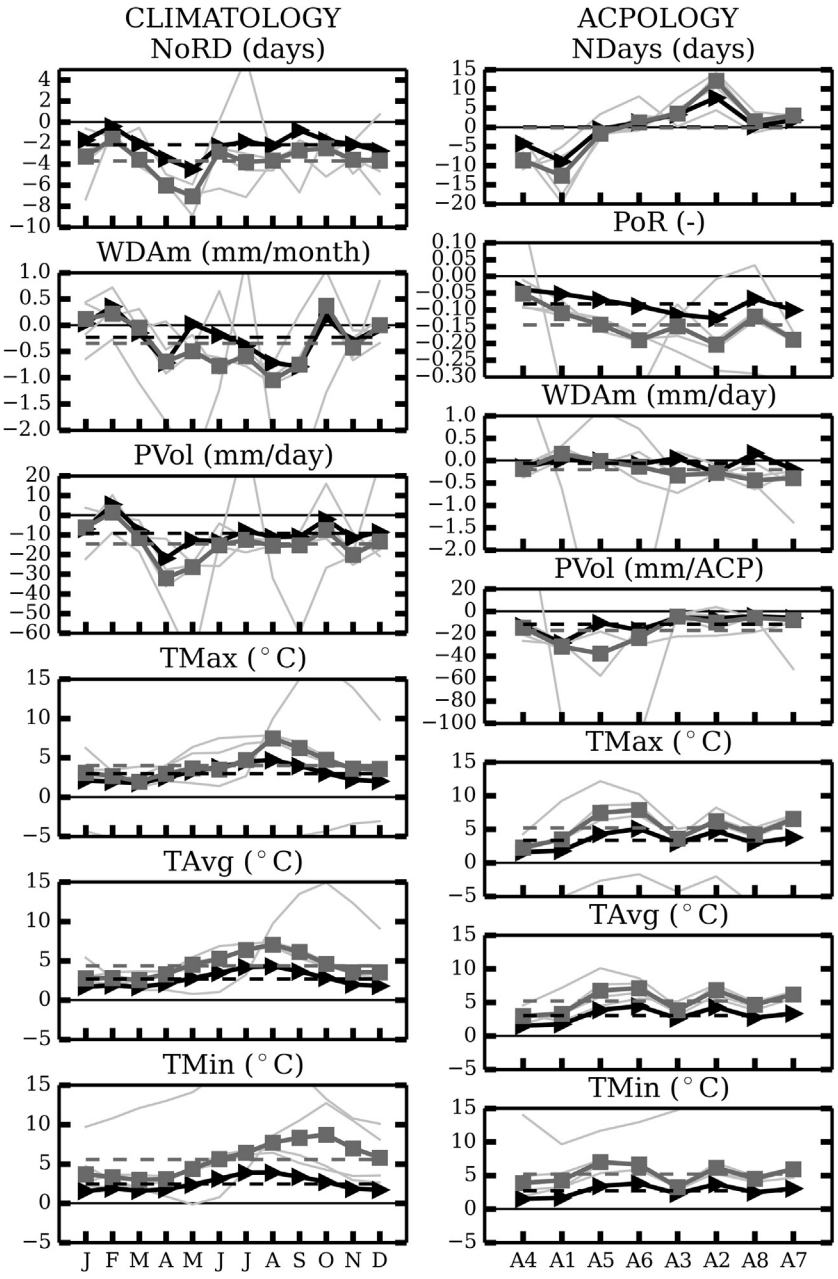

Fig. 13. Analysis of Projected Changes in Climatology (left column) and ACPology (right column) from 40-year historical period (1960–1999) to 40-year future period (2060–2099). Legend information is as provided for Fig. 10.

per year from an initial 64) and with little difference between the RCP scenarios, A5, A6 and A3 showing practically no change, and A2, A8 and A7 showing increases. The most marked change is for A2 (directional N/NE; that brings the cold and dry '*Tramuntana*' winds) with an increase of 16 days per year from an initial 48 days.

Perhaps more important from the point of view of a water resources assessment are the projected changes in Number of Rainy Days (*NoRD*) and Wet day Amount (*WDAm*). Here we see marked declines in *NoRD* for the fine weather system A4 (22 days from an initial 70), the wet directional A1 system out of the North and West (17 days from an initial 57), and the wet cyclonic A5 and A6 systems (together 14 days from an initial 48). However, the model ensemble projections of *WDAm* are quite variable, with the median projections indicating either none or only moderate reductions over the period, except perhaps for the projected declines for the cyclonic A5 and A6 that seem somewhat more definitive. Overall, the projections suggest that the projected reductions in mean annual Precipitation Volume (~130 mm/year) reported above will occur mainly for A1 (~45%), A5 (~30%) and A6 (~25%).

4.3. Projected changes in climatology and ACPology

Finally, we evaluate GCMs projections for potential changes in the average hydro-climatology of the Upper Guadiana Basin, and regarding changes to the frequency distribution and properties of the atmospheric circulation patterns. For this we compute the '*climatology*' and '*ACPology*' for the historical 40-year period (1960–1999) and for the future 40-year period (2060–2099), and compute the differences. The results are reported in Figs. 13 and 14.

The left column of Fig. 13 indicates that temperatures will increase more during the summer (4–7 °C) than during the winter (2–3 °C), the Number of Rainy Days will decrease on average by about 2–3 days per month, with larger declines in April and May (4–7 days/month), and Wet Day Amounts will decline mainly in April and in the summer. These, however, are the result of changes in the frequencies and hydro-climatological properties of the circulation patterns. The right column of Fig. 13 shows that substantial declines can be seen in the frequency of A4 (anti-cyclonic high pressure) and A1 (directional N/NW/W/SW) indicating fewer fine-weather A4 days (4–8 days/year) and A1 systems bringing

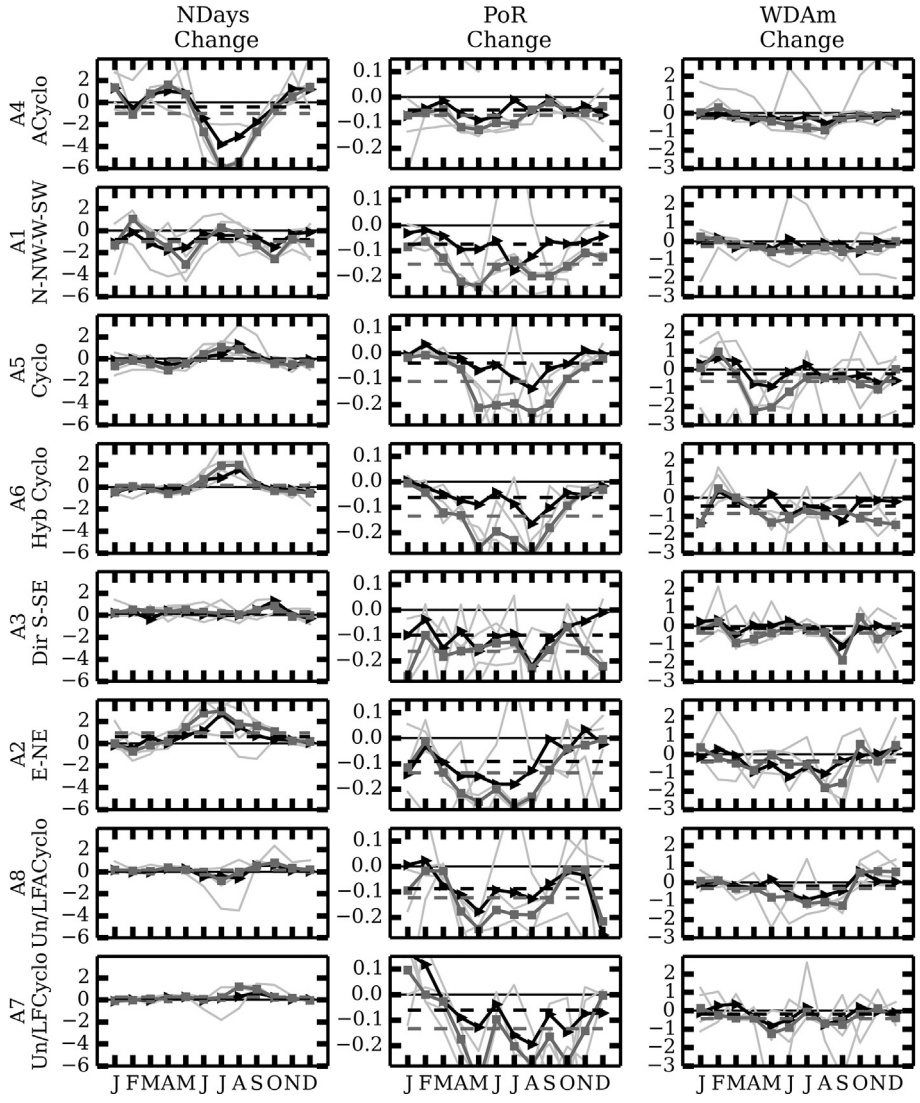

Fig. 14. Analysis of Projected Changes in ACP-Climatology, from 40-year historical period (1960–1999) to 40-year future period (2060–2099). First column is for the Number of ACP Days (*NDays*), second column is for the Probability of Rain (*PoR*), and third column is for the Wet Day Amount (*WDAm*). Legend information is as provided for Fig. 10.

moisture from the Atlantic Ocean and Cantabric Sea (11–19 days/year). At the same time, we can expect marked increases in dry A2 days (8–12 days/year), and moderate increases in the other systems.

In general the results suggest small or moderate declines in Wet Day Amounts across the systems, so that the main causes of declines in Precipitation Volume are changes in the Number of ACP Days, and declines in the corresponding Probabilities of Rain (5–15%); the latter can be seen to be generally larger for systems experiencing greater warming.

Details of projected climatological changes to each ACP are presented in Fig. 14. For the Number of ACP days per month (*NDays*), strong effects are projected for the fine weather A4 system (anti-cyclonic; significant declines in summer frequency and slight increases in winter frequency), and for the directional A2 system (E/NE; notable increases in summer frequency). The A1 (directional N/NW/W/SW) system shows declines in spring and fall, while the A5 and A6 (cyclonic) systems show moderate summer increases, and the remaining show little change. However, Probability of Rain (*PoR*) shows substantial declines across all systems, with larger declines during the warmer summer months, and Wet Day Amount (*WDAm*) shows only moderate climatological effects.

5. Conclusions and discussion

The paper reports an approach to assessing local catchment-scale hydro- meteorological impacts of projected climate change based on the fact that GCMs do a better job at simulating the properties of atmospheric circulation patterns (ACPs) than they do for precipitation amount. To illustrate the approach, we present results for the 16,000 km^2 Upper Guadiana Basin in central Spain. We show that while the twenty GCMs participating in the most recent (5th) IPCC Assessment are generally very poor at simulating the magnitudes and climatological patterns of Wet Day Amount (and hence Precipitation Volume), most of them actually display remarkably good performance with respect to the ACPology, that is, the frequency distribution of ACP types and their climatological properties, such as Number of Rainy Days and Probability of Rain (Figs. 2 and 5).

Further, only four of the twenty GCMs provide reasonably satisfactory agreement with historical observations of temperature and rainfall variables, as measured by the mean level and shape correlation in terms of Climatology and ACPology for the Upper Guadiana Basin (Figs. 7 and 8).

Based on this, we examined the hydro-climatic trends projected by the selected ensemble of four GCMs for the Upper Guadiana Basin, for two of the greenhouse gas emissions scenarios (RCP 4.5 and RCP 8.5; representing moderate and strong increases in radiation pathways) recommended by the 5th IPCC Assessment report. Results for the adjusted climate variables indicate that temperature (*Max*, *Avg*. and *Min*) increases regardless of the RCP scenario. Meanwhile, the number of rainy days and the precipitation volume decrease for ACPs 1 and 4. These changes are more marked for the observation data than for GCMs outputs.

Note that ACP1 corresponds to the typical cyclonic circulation pattern that brings moisture from the Atlantic Ocean and Cantabric Sea, and which is characterized by stratiform frontal rain with large spatial continuity and duration. In contrast, ACP4 corresponds to an anti-cyclonic circulation pattern that is typically accompanied by fine weather, and which is characterized by small convective rain cells of short duration and small precipitation volume. Given the high frequency of occurrence of ACP4, a reduction in associated precipitation volume could prove serious to the shrubs and other small plants that survive the otherwise arid summers in this area.

Further, we analyzed the projected changes in climatology and ACPology between the latter 40 years of the 20th Century and the 21st Century. Results show a clear reduction in frequency of low-pressure fronts coming from the Atlantic Ocean and the Cantabric Sea. As a result there is a reduction in both the Number of Rainy Days and the Precipitation Volume (but not in the Wet-Day Amount). More importantly, the observed trend of change is faster than simulated by GCMs, which is consistent with observations around the Mediterranean region (e.g., Norrant-Romand and Douguédroit, 2014).

In general, our results suggest a relatively simple alternative to the commonly applied strategy of precipitation bias correction by statistical downscaling and bias correction, and rely upon the ability of GCMs to provide relatively good simulations of the time-evolution of atmospheric circulation patterns and their associated probabilities of rain. Observed data (e.g., precipitation and temperature measurements at several gauges with sufficiently long records) can then be used to compute simple correction factors for mean Wet Day Amounts associated with various ACPs (thereby accounting for differing interactions between atmospheric flows and local topography effects). The only real additional complexity involved in this method is the classification of ACPs (Jones et al., 2013).

Further, our approach is consistent with the method developed by Sapriza-Azuri et al. (2013) for stochastic generation of spatio-temporally non-stationary rainfall fields. This requires the time history (daily sequence) of ACPs, whether it rains or not (anywhere within the basin), and the basin-scale mean wet day precipitation amounts. For hindcasting, these data can be provided by an analysis of historical data and/or simulations provided by regional weather forecasting models. For future projections, they can be obtained from information provided by GCMs, with adjustments (bias correction) such as discussed in this paper. In the case of catchment-scale lumped hydrological modeling, the forcing data (daily ACP type, Rain/No-Rain indicator, and Wet Day Amount) can be used directly, whereas for spatially distributed hydrological modeling the information can be used to drive the set of SRGPs described above.

As mentioned earlier any assessment of future climate impacts must make several important assumptions. We have verified here that the current suite of GCMs is capable of providing sufficiently accurate simulations of atmospheric circulation patterns, probabilities of rain, and temperature under current conditions (AS1), while being poor at simulating Wet Day Amount. The results of a climate impact assessment depend, therefore, on the (currently untestable) assumptions that: (a) GCMs can provide sufficiently accurate estimates of the evolution of hydro-climatological variable under future potential emission scenarios (AS2); and (b) Other properties of the local rainfall generation mechanism (spatial probability distributions and interactions with elevation) are not substantially altered (AS3). Of course, while we have focused here mainly on mean Wet Day Amount, one would also generally be interested in the shape of the daily probability distribution of Wet Day Amount, which will altered by changes in the probability of extreme intensity precipitation (the upper tails of the distribution). In future work, we will extend our investigation to explore such effects.

Another aspect of interest is the long term (multi-year) periodic cycles associated with droughts (and also wet spells). Since these are necessarily associated with changes in global (and hence regional) atmospheric circulation and associated precipitation mechanisms, the approach presented here has the potential to provide further insight into how future cycles of wet and dry periods might be impacted (at the local scale) by increasing greenhouse concentrations, thereby providing enhanced information for use by water resources managers and planners. While we have focused in this

paper primarily on climatological (long-term) behaviors and trends, an analysis of patterns of temporal evolution (and cycles therein) is also possible, and is planned for future investigation.

Conflict of interest

The authors declare that there are no conflicts of interest.

Acknowledgments

The first author received sabbatical support from the Spanish Ministry of Science and Innovation (MEC), and also partial support from the Australian Research Council through the Centre of Excellence for Climate System Science (grant number CE110001028), the Cooperative Research Programme (Trade and Agriculture) of the Organization for European Co-Operation and Development (OECD), and the EU-funded project '*Sustainable Water Action (SWAN): Building Research Links Between EU and US*' (INCO-20011-7.6 grant number 294947). The second, third and fourth authors were supported by a European Union (FP6) funded Integrated Project called WATCH through contract number 036946. The meteorological data were provided by the Spanish state meteorological agency (AEMET). Support of the Guadiana Water Authority (Confederación Hidrográfica del Guadiana) through its President, José Díaz Mora, is also acknowledged.

References

Anagnostopoulos, G.G., Koutsoyiannis, D., Christofides, A., Efstratiadis, A., Mamassis, N., 2010. A comparison of local and aggregated climate model outputs with observed data. Hydrol. Sci. J. 55 (7), 1094–1110. http://dx.doi.org/10.1080/02626667.2010.513518.

Bardossy, A., Plate, E.J., 1992. Space-time model for daily rainfall using atmospheric circulation patterns. Water Resour. Res. 28 (5), 1247–1259.

Bárdossy, A., Pegram, G., 2011. Downscaling precipitation using regional climate models and circulation patterns toward hydrology. Water Resour. Res. 47 (4).

Brekke, L.D., Dettinger, M.D., Maurer, E.P., Anderson, M., 2008. Significance of model credibility in estimating climate projection distributions for regional hydroclimatological risk assessments". Clim. Change 89 (3–4), 371–394.

Bronstert, A., Kolokotronis, V., Schwandt, D., Straub, H., 2007. Comparison and evaluation of regional climate scenarios for hydrological impact analysis: general scheme and application example. Int. J. Climatol. 27 (12), 1579–1594. http://dx.doi.org/10.1002/joc.1621.

Dai, A., 2006. Precipitation characteristics in eighteen coupled climate models. J. Clim. 19 (18), 4605–4630. http://dx.doi.org/10.1175/JCLI3884.1.

Demuzere, M., Trigo, R.M., Vila-Guerau de Arellano, J., Van Lipzig, N.P.M., 2009. The impact of weather and atmospheric circulation on O 3 and PM 10 levels at a rural mid-latitude site. Atmos. Chem. Phys. 9 (8), 2695–2714.

Déqué, M., Rowell, D., Lüthi, D., Giorgi, F., Christensen, J., Rockel, B., Jacob, D., Kjellström, E., deCastro, M., vanden Hurk, B., 2007. An intercomparison of regional climate simulations for Europe: assessing uncertainties in model projections. Clim. Change 81 (S1), 53–70. http://dx.doi.org/10.1007/s10584-006-9228-x.

Dominguez, F., Canon, J., Valdes, J., 2010. IPCC-AR4 climate simulations for the Southwestern US: the importance of future ENSO projections. Clim. Change 99 (3–4), 499–514.

Esteban, P., Jones, P.D., Martin-Vide, J., Mases, M., 2005. Atmospheric circulation patterns related to heavy snowfall days in Andorra, Pyrenees. Int. J. Climatol. 25 (3), 319–329.

Fowler, H.J., Blenkinsop, S., Tebaldi, C., 2007. Linking climate change modelling to impacts studies: recent advances in downscaling techniques for hydrological modelling. Int. J. Climatol. 27 (12), 1547–1578.

Goodess, C.M., Jones, P.D., 2002. Links between circulation and changes in the characteristics of Iberian rainfall. Int. J. Climatol. 22, 1593–1615. http://dx.doi.org/10.1002/joc.810.

Goodess, C.M., Palutikof, J.P., 1998. Development of daily rainfall scenarios for southeast Spain using a circulation-type approach to downscaling. Int. J. Climatol. 18 (10), 1051–1083.

Haberlandt, U., Belli, A., Bárdossy, A., 2014. Statistical downscaling of precipitation using a stochastic rainfall model conditioned on circulation patterns – an evaluation of assumptions. Int. J. Climatol. http://dx.doi.org/10.1002/joc.3989.

Huth, R., Beck, C., Philipp, A., Demuzere, M., Ustrnul, Z., Cahynová, M., Kyselý, J., Tveito, O.E., 2008. Classifications of atmospheric circulation patterns. Ann. N. Y. Acad. Sci. 1146, 105–152. http://dx.doi.org/10.1196/annals.1446.019.

IPCC, 2000. Special Report on Emissions Scenarios, Edited by Nebojsa Nakicenovic and Robert Swart. Cambridge University Press, Cambridge, UK, July 2000, 1, pp. 612. ISBN 0521804930.

IPPC, 2001. In: Houghton, J.T. et al. (Eds.), Climate Change 2001: The Scientific Basis. The Contribution of Working Group I to the Third Assessment Report of the Intergovernmental Panel on Climate Change. Cambridge Univ. Press, New York.

IPCC, 2007. In: Solomon, S., Qin, D., Manning, M., Chen, Z., Marquis, M., Averyt, K.B., Tignor, M., Miller, H.L. (Eds.), Climate Change 2007: The Physical Science Basis. Contribution of Working Group I to the Fourth Assessment Report of the Intergovernmental Panel on Climate Change. Cambridge University Press, Cambridge, United Kingdom and New York, NY, USA.

IPCC, 2013. Climate Change 2013: The Physical Science Basis. Contribution of Working Group I to the Five Assessment Report of the Intergovernmental Panel on Climate Change.

Jenkinson, A., Collison, F., 1977. An initial climatology of gales over the North Sea. Synoptic Climatol. Branch Memorandum 62.

Johnson, F., Sharma, A., 2009. Measurement of GCM skill in predicting variables relevant for hydroclimatological assessments. J. Clim. 22 (16), 4373–4382. http://dx.doi.org/10.1175/2009JCLI2681.1.

Johnson, F., Sharma, A., 2011. Accounting for interannual variability: a comparison of options for water resources climate change impact assessments. Water Resour. Res. 47 (4). http://dx.doi.org/10.1029/2010WR009272.

Johnson, F., Sharma, A., 2012. A nesting model for bias correction of variability at multiple time scales in general circulation model precipitation simulations. Water Resour. Res. 48 (W01504), 16. http://dx.doi.org/10.1029/2011WR010464.

Jones, P.D., Hulme, M., Briffa, K.R., 1993. A comparison of Lamb circulation types with an objective classification scheme. Int. J. Climatol. 13 (6), 655–663. http://dx.doi.org/10.1002/joc.3370130606.

Jones, P.D., Harpham, C., Briffa, K.R., 2013. Lamb weather types derived from reanalysis products. Int. J. Climatol. 33, 1129–1139. http://dx.doi.org/10.1002/joc.3498.

Kalnay, E., Kanamitsu, M., Kistler, R., Collins, W., Deaven, D., Gandin, L., et al., 1996. The NCEP/NCAR 40-year reanalysis project. Bull. Am. Meteorol. Soc. 77 (3), 437–471.

Kundzewicz, Z.W., Mata, L.J., Arnell, N.W., Döll, P., Jimenez, B., Miller, K., Oki, T., Shiklomanov, I., 2008. The implications of projected climate change for freshwater resources and their management. Hydrol. Sci. J. 53 (1), 3–10.

Lambán, L.J., Jódar, J., Custodio, E., Soler, A., Sapriza, G., Soto, R., 2015. Isotopic and hydrogeochemical characterization of high-altitude karst aquifers in complex geological settings. The Ordesa and Monte Perdido National Park (Northern Spain) case study. Sci. Total Environ. 506, 466–479. http://dx.doi.org/10.1016/j.scitotenv.2014.11.030.

Lee, C.C., Sheridan, S.C., 2011. A six-step approach to developing future synoptic classifications based on GCM output. Int. J. Climatol. 32, 1792–1802. http://dx.doi.org/10.1002/joc.2394.

Lionello, P., Abrantes, F., Gacic, M., Planton, S., Trigo, R., Ulbrich, U., 2014. The climate of the Mediterranean region: research progress and climate change impacts. Reg. Environ. Change 14 (5), 1679–1684.

Maurer, E.P., 2007. Uncertainty in hydrologic impacts of climate change in the Sierra Nevada, California under two emissions scenarios. Clim. Change 82 (3–4), 309–325.

Moss, R.H., Edmonds, J.A., Hibbard, K.A., Manning, M.R., Rose, S.K., van Vuuren, D.P., Carter, T.R., Emori, S., Kainuma, M., Kram, T., Meehl, G.A., Mitchell, J.F.B., Nakicenovic, N., Riahi, K., Smith, S.J., Stouffer, R.J., Thomson, A.M., Weyant, J.P., Wilbanks, T.J., 2010. The next generation of scenarios for climate change research and assessment. Nature 463, 747–756. http://dx.doi.org/10.1038/nature08823.

Norrant-Romand, C., Douguédroit, A., 2014. Significant rainfall decreases and variations of the atmospheric circulation in the Mediterranean (1950–2000). Reg. Environ. Change 14 (5), 1725–1741.

Piani, C., Weedon, G., Best, M., Gomes, S., Viterbo, P., Hagemann, S., et al., 2010. Statistical bias correction of global simulated daily precipitation and temperature for the application of hydrological models. J. Hydrol. 395 (3–4), 199–215. http://dx.doi.org/10.1016/j.jhydrol.2010.10.024.

Piao, S., Ciais, P., Huang, Y., Shen, Z., Peng, S., Li, J., Fang, J., 2010. The impacts of climate change on water resources and agriculture in China. Nature 467 (7311), 43–51.

Pierce, D.W., Barnett, T.P., Santer, B.D., Gleckler, P.J., 2009. Selecting global climate models for regional climate change studies. Proc. Natl. Acad. Sci. USA 106 (21), 8441–8446.

Randall, D.A., Wood, R.A., Bony, S., Colman, R., Fichefet, T., Fyfe, J., Kattsov, V., Pitman, A., Shukla, J., Srinivasan, J., Stouffer, R.J., Sumi, A., Taylor, K.E., 2007. Cilmate models and their evaluation. In: Solomon, S., Qin, D., Manning, M., Chen, Z., Marquis, M., Averyt, K.B., Tignor, M., Miller, H.L. (Eds.), Climate Change 2007: The Physical Science Basis. Contribution of Working Group I to the Fourth Assessment Report of the Intergovernmental Panel on Climate Change. Cambridge University Press, Cambridge.

Sapriza-Azuri, G., Jódar, J., Carrera, J., Gupta, H., 2013. Stochastic simulation of nonstationary rainfall fields, accounting for seasonality and atmospheric circulation pattern evolution. Math. Geosci. 45 (5), 621–645. http://dx.doi.org/10.1007/s11004-013-9467-0.

Sapriza Azuri, Gonzalo, 2013. A Methodology to Assess the Combined Effect of Climate Change and Groundwater Overexploitation over the Upper Guadiana Basin, Spain. Doctoral Thesis. Universitat Politècnica de Catalunya. Departament d'Enginyeria del Terreny, Cartogràfica i Geofísica. Thesis link: <http://hdl.handle.net/10803/135003>.

Sapriza-Azuri, G., Jodar, J., Navarro, V., Slooten, L.J., Carrera, J., Gupta, H., 2015. Impacts of rainfall spatial variability on hydrogeological response. Water Resour. Res. http://dx.doi.org/10.1002/2014WR016168.

Sheridan, S.C., Lee, C.C., 2010. Synoptic climatology and the general circulation model. Prog. Phys. Geogr. 34, 101–109.
Sivakumar, B., 2011. Global climate change and its impacts on water resources planning and management: assessment and challenges. Stochastic Environ. Res. Risk Assess. 25 (4), 583–600. http://dx.doi.org/10.1007/s00477-010-0423-y.
Stahl, K., Moore, R.D., McKendry, I.G., 2006. Climatology of winter cold spells in relation to mountain pine beetle mortality in British Columbia, Canada. Clim. Res. 32 (1), 13–23.
Taylor, K.E., Stouffer, R.J., Meehl, G.A., 2011. An overview of CMIP5 and the experiment design. Bull. Am. Meteorol. Soc. 93 (4), 485–498. http://dx.doi.org/10.1175/BAMS-D-11-00094.1.
van Vuuren, D.P., Edmonds, J., Kainuma, M., Riahi, K., Thomson, A., Hibbard, K., Hurtt, G.C., Kram, T., Krey, V., Lamarque, J.F., Masui, T., Meinshausen, M., Nakicenovic, N., Smith, S.J., Rose, S.K., 2011. The representative concentration pathways: an overview. Clim. Change 109 (1–2), 5–31.
Vicente-Serrano, S.M., López-Moreno, J.I., 2006. The influence of atmospheric circulation at different spatial scales on winter drought variability through a semi-arid climatic gradient in Northeast Spain. Int. J. Climatol. 26 (11), 1427–1453.
Wi, S., Dominguez, F., Durcik, M., Valdes, J., Diaz, H.F., Castro, C.L., 2012. Climate change projection of snowfall in the Colorado River Basin using dynamical downscaling. Water Resour. Res. 48 (5).
Woldemeskel, F.M., Sharma, A., Sivakumar, B., Mehrotra, R., 2012. An error estimation method for precipitation and temperature projections for future climates. J. Geophys. Res. – Atmos. 117. http://dx.doi.org/10.1029/2012jd018062 Artn D22104.
Wood, A.W., Maurer, E.P., Kumar, A., Lettenmaier, D.P., 2002. Long-range experimental hydrologic forecasting for the eastern United States. J. Geophys. Res. – Atmos. 107 (D20).
Wood, A.W., Leung, L.R., Sridhar, V., Lettenmaier, D.P., 2004. Hydrologic implications of dynamical and statistical approaches to downscaling climate model outputs. Clim. Change 62 (1–3), 189–216.
Xoplaki, E., Trigo, et al., 2012. Large-scale atmospheric circulation driving extreme climate events in the Mediterranean and its related impacts. Clim. Mediterranean Reg., 347–417